Molecular Pharmacology Fast Forward. Published on September 16, 2020 as DOI: 10.1124/molpharm.120.000048
This article has not been copyedited and formatted. The final version may differ from this version.

GS-967 and Eleclazine Block Sodium Channels in Human Induced Pluripotent Stem Cell-derived Cardiomyocytes

MOLPHARM-AR-2020-000048 2nd Revision

Franck Potet, Defne E. Egecioglu, Paul W. Burridge, and Alfred L. George, Jr.

Department of Pharmacology, Northwestern University Feinberg School of Medicine, Chicago, IL 60611

Molecular Pharmacology Fast Forward. Published on September 16, 2020 as DOI: 10.1124/molpharm.120.000048
This article has not been copyedited and formatted. The final version may differ from this version.

Running Title: *Cardiac sodium channel block by GS-967 and eleclazine*

To whom correspondence should be addressed:

Alfred L. George, Jr.
Department of Pharmacology
Northwestern University Feinberg School of Medicine
Searle 8-510
320 East Superior Street
Chicago, IL 60611
Tel: 312-503-4893
al.george@northwestern.edu

The number of text pages: 33
Number of tables: 1
Number of figures: 5
Number of references: 41
The number of words in the *Abstract:* 216
The number of words in the *Introduction*: 635
The number of words in the *Discussion*: 879

Molecular Pharmacology Fast Forward. Published on September 16, 2020 as DOI: 10.1124/molpharm.120.000048
This article has not been copyedited and formatted. The final version may differ from this version.

ABBREVIATIONS

Na_V: voltage gated sodium channel

GS-967: GS-458967

UDB: use-dependent block

I_{NaP}: peak sodium current

I_{NaL}: late sodium current

DMEM: Dulbecco's modified eagle medium

DPBS: Dulbecco's phosphate-buffered saline

FBS: fetal bovine serum

LQTS: long QT syndrome

HEPES: 4-(2-hydroxyethyl)-1-piperazineethanesulfonic acid

SEM: standard error of the mean

SD: standard deviation

IC_{50}: half maximal inhibitory concentration

tsA201: transformed human embryonic kidney 293 cells

hiPSC: human induced pluripotent stem cell

CDM3: chemically defined medium 3

K_{ON}: binding rate

K_{OFF}: unbinding rate

95% CI: 95% confidence interval

Molecular Pharmacology Fast Forward. Published on September 16, 2020 as DOI: 10.1124/molpharm.120.000048
This article has not been copyedited and formatted. The final version may differ from this version.

ABSTRACT

GS-967 and eleclazine (GS-6615) are novel sodium channel inhibitors exhibiting antiarrhythmic effects in various *in vitro* and *in vivo* models. The antiarrhythmic mechanism has been attributed to preferential suppression of late sodium current (I_{NaL}). Here, we took advantage of a throughput automated electrophysiology platform (SyncroPatch 768PE) to investigate the molecular pharmacology of GS-967 and eleclazine on peak sodium current (I_{NaP}) recorded from human induced pluripotent stem cell (hiPSC)-derived cardiomyocytes. We compared the effects of GS-967 and eleclazine to the antiarrhythmic drug lidocaine, the prototype I_{NaL} inhibitor ranolazine, and the slow inactivation enhancing drug lacosamide. In human induced pluripotent stem cell-derived cardiomyocytes, GS-967 and eleclazine caused a reduction of I_{NaP} in a frequency-dependent manner consistent with use-dependent block (UDB). GS-967 and eleclazine had similar efficacy but evoked more potent UDB of I_{NaP} (IC_{50}=0.07 and 0.6 μM, respectively) than ranolazine (7.8 μM), lidocaine (133.5 μM) and lacosamide (158.5 μM). In addition, GS-967 and eleclazine exerted more potent effects on slow inactivation and recovery from inactivation compared to the other sodium channel blocking drugs we tested. The greater UDB potency of GS-967 and eleclazine was attributed to the higher association rates (K_{ON}) and moderate unbinding rate (K_{OFF}) of these two compounds with sodium channels. We propose that substantial UDB contributes to the observed antiarrhythmic efficacy of GS-967 and eleclazine.

Molecular Pharmacology Fast Forward. Published on September 16, 2020 as DOI: 10.1124/molpharm.120.000048
This article has not been copyedited and formatted. The final version may differ from this version.

SIGNIFICANCE STATEMENT

We investigated the molecular pharmacology of GS-967 and eleclazine on sodium channels in human induced pluripotent stem cell derived cardiomyocytes using a high throughput automated electrophysiology platform. Sodium channel inhibition by GS-967 and eleclazine has unique effects including accelerating the onset of slow inactivation and impairing recovery from inactivation. These effects combined with rapid binding and moderate unbinding kinetics explain potent use-dependent block, which we propose contributes to their observed antiarrhythmic efficacy.

Molecular Pharmacology Fast Forward. Published on September 16, 2020 as DOI: 10.1124/molpharm.120.000048
This article has not been copyedited and formatted. The final version may differ from this version.

INTRODUCTION

Sodium current (I_{Na}) in cardiac myocytes carried primarily by $Na_V1.5$ channels is responsible for the rapid upstroke of atrial and ventricular action potentials as well as the rapid propagation of depolarization throughout the heart. Sodium channels can transition between at least three distinct states: resting (closed), open (active) and inactivated (non-conducting) (Hodgkin and Huxley, 1952). The transitions between these states are voltage and time dependent. Antiarrhythmic, anticonvulsant and local anesthetic agents have been shown to block the propagation of action potentials by interacting differently with each channel state (Strichartz et al., 1987). In cardiac tissue, the main effect of antiarrhythmic drugs is to prevent abnormal electrical impulse propagation and conduction, thus suppressing non-pacemaker generated electrical activity arising from damaged cardiac myocytes.

Effective class I antiarrhythmic drugs such as lidocaine, which block voltage-gated sodium channels, exhibit greater efficacy in situations associated with rapid repetitive firing of action potentials (use-dependent block) or prolonged tissue depolarization, such as in myocardial ischemia. Thus, effective arrhythmia suppression depends on the properties of the drug molecule that convey high affinity binding to the channel pore when the channel is in the open or inactivated state. Such high affinity binding results in a slowed recovery of the drug-bound channel from inactivation as the cell membrane repolarizes (Ragsdale et al., 1996).

Molecular Pharmacology Fast Forward. Published on September 16, 2020 as DOI: 10.1124/molpharm.120.000048
This article has not been copyedited and formatted. The final version may differ from this version.

Disturbances in $Na_V1.5$ function can promote life-threatening cardiac arrhythmia. When $Na_V1.5$ fails to inactivate fully after opening, Na^+ influx continues throughout the action potential plateau. The resulting current, referred as late I_{Na} (I_{NaL}), can promote prolongation of the action potential duration. Late I_{Na} is normally small, but its amplitude is greater in certain acquired or heritable conditions, including failing and/or ischemic heart (Le Grand et al., 1995), oxidative stress (Song et al., 2006), or mutations in *SCN5A*, which encodes $Na_V1.5$ (Bennett et al., 1995; Ruan et al., 2009). *SCN5A* mutations that cause enhanced I_{NaL} produce type 3 long QT syndrome (LQT3) (Antzelevitch et al., 2014). Drugs that selectively suppress I_{NaL} may offer a targeted antiarrhythmic strategy in these conditions.

Many local anesthetic and antiarrhythmic agents have greater potency to block I_{NaL} than peak I_{Na} (I_{NaP}). Certain compounds such as ranolazine (Gupta et al., 2015) and F15845 (Pignier et al., 2010), are described as preferential I_{NaL} blockers. GS-967 (a triazolopyridine derivative, 6-(4-(trifluoromethoxy)phenyl)-3-(trifluoromethyl)-[1,2,4]triazolo[4,3-a]pyridine also referred as PRAX-330) (Koltun et al., 2016) and eleclazine (dihydrobenzoxazepinone, formerly known as GS-6615) are recently described sodium channel blockers that were originally demonstrated to exert potent antiarrhythmic effects in rabbit ventricular, canine and pig atrial myocytes by a proposed mechanism of action involving preferential I_{NaL} block (Belardinelli et al., 2013; Fuller et al., 2016; Sicouri et al., 2013). We previously demonstrated that GS-967, in addition to blocking I_{NaL}, also exerts a strong use-dependent block (UDB) of I_{NaP} conducted by heterologously expressed recombinant human $Na_V1.5$ and proposed that this

Molecular Pharmacology Fast Forward. Published on September 16, 2020 as DOI: 10.1124/molpharm.120.000048
This article has not been copyedited and formatted. The final version may differ from this version.

phenomenon might contribute to its antiarrhythmic effect (Potet et al., 2016). Further studies examining the molecular pharmacology of GS-967 and eleclazine on sodium channels in cardiomyocytes should provide valuable insight into the drugs' mechanism of action in a therapeutically relevant environment.

In this study, we investigated the molecular pharmacology of GS-967 and eleclazine in hiPSC-derived cardiomyocytes using a high throughput automated electrophysiology platform (SyncroPatch 768PE). We compared GS-967 and eleclazine to lidocaine (a class 1-b antiarrhythmic drug that promotes UDB) (Herzog et al., 2003), to ranolazine (a prototype I_{NaL} inhibitor with class1-b antiarrhythmic characteristics) (Szel et al., 2011), and to lacosamide (an anticonvulsant drug that enhances slow inactivation) (Errington et al., 2008). Both, ranolazine and lacosamide can enhance slow inactivation of Na_V channels (Errington et al., 2008; Kahlig et al., 2014). We observed that eleclazine, like GS-967, exhibit moderate dissociation rates, comparable to the class 1-b antiarrhythmic lidocaine, along with uniquely rapid binding kinetics. These properties explain the potent use-dependent block of I_{NaP} by GS-967 and eleclazine observed in hiPSC-derived cardiomyocytes.

Molecular Pharmacology Fast Forward. Published on September 16, 2020 as DOI: 10.1124/molpharm.120.000048
This article has not been copyedited and formatted. The final version may differ from this version.

MATERIALS AND METHODS

Cell Culture

Human iPSC were derived from peripheral blood of a male donor as previously described (Burridge et al., 2016). The resulting line was designated 113c4. The hiPSC line was cultured on growth factor-reduced Matrigel (Corning, NY, USA) in E8 medium (Burridge et al., 2015). Cardiac differentiation was completed in CDM3 as previously described (Burridge et al., 2014). CDM3 consisted of RPMI 1640 (Corning), 500 µg/ml fatty acid-free albumin (GenDEPOT, Barker, TX, USA), and 200 µg/ml L-ascorbic acid 2-phosphate (Wako, Richmond, VA, USA). At day 20 (d20) of differentiation, cells were dissociated by incubation in DPBS (without Mg^{2+} or Ca^{2+}) for 20 min at 37°C and then in 1:200 Liberase TH (Roche, Basel, Switzerland) in DPBS for 20 min at 37°C. Cells were collected by centrifuging at 200 $\times g$ for 3 min, counted, then replated in Matrigel-coated 6-well plates at 2-4 million cells per well in CDM3 supplemented with 40% FBS (Opti-Gold, GenDEPOT, Katy, TX, USA). Cells were returned to CDM3 on d22. Human iPSC-derived cardiomyocytes were re-plated in 30 mm culture dishes 5 days prior to the experiment.

Automated patch clamp recording

Automated patch clamp recording was performed using a Syncropatch 768 PE (Nanion Technologies, Munich, Germany). On the day of the experiment, cells were washed once with DPBS (Mg/Ca free) for 20 minutes. Cells were then detached with 5 min treatment with TrypLE followed by 20-30 minutes treatment with CDM3 media with 1:200 dilution of Liberase TH. Cells were then re-suspended in 15% CDM3 media and

Molecular Pharmacology Fast Forward. Published on September 16, 2020 as DOI: 10.1124/molpharm.120.000048
This article has not been copyedited and formatted. The final version may differ from this version.

85% external solution at 170,000 cells/ml. Cells were allowed to recover for at least 30 min at 15°C while shaking on a rotating platform. Following equilibration, 10 µl of cell suspension was added to each well of a 384-well, single-hole, low resistance (3 MΩ) NPC-384 'chip' (Nanion Technologies).

Pulse generation and data collection were done with PatchController384 V.1.3.0 and DataController384 V1.2.1 (Nanion Technologies). Whole-cell currents were filtered at 3 kHz and acquired at 10 kHz. The access resistance and apparent membrane capacitance were estimated using protocols within the data acquisition software. Series resistance was compensated 95% and leak and capacitance artifacts were subtracted out using the P/4 method. Whole-cell currents were recorded at room temperature (~ 24°C) in the whole-cell configuration. The external solution contained (in mM): NaCl 140, KCl 4, $CaCl_2$ 2, $MgCl_2$ 1, HEPES 10, glucose 5, pH = 7.4. The internal solution contained (in mM): CsF 110, CsCl 10, NaCl 10, HEPES 10, EGTA 20, pH = 7.2.

Using hiPSC-derived cardiomyocytes, the average cell catch per plate was 58 ± 4% of wells (ranging from 22-84%). The average number of cells per plate with a seal resistance >0.25 GΩ was 48 ± 5% (range 11-80%), and among these cells 56 ± 4% (range 12-91%) expressed sodium current. Only cells with good voltage control and a peak current ≥300 pA were selected for analysis. Using these criteria, the success rate of recording sodium current from hiPSC-derived cardiomyocytes was 25 ± 2% of wells. The average seal resistance of the cells selected for analysis was 0.618 ± 0.05 GΩ and

Molecular Pharmacology Fast Forward. Published on September 16, 2020 as DOI: 10.1124/molpharm.120.000048
This article has not been copyedited and formatted. The final version may differ from this version.

the average capacitance was 18.3 ± 0.7 pF. The average access resistance was 5.6 MΩ, and the calculated voltage error was 3.2 mV.

Drugs were diluted in the external solution and prepared in a separate 24 well plate. GS-967 was obtained from Gilead (Foster City, CA). Eleclazine, lidocaine, ranolazine and lacosamide were obtained from Sigma Aldrich (St. Louis, MO). DMSO concentration was the same for each concentration of a given drug. To block voltage-gated Ca^{2+} channels, 0.5 μM nisoldipine (Sigma Aldrich; St. Louis, MO) was added to external solutions.

Data analysis

Cells were excluded from analysis if the maximum peak current was less than 300 pA, which was a pre-determined threshold. Patch-clamp measurements are presented as means ± SD or SEM (used for clarity in data-dense plots). Half maximal inhibitory concentration (IC_{50}) values were calculated by fitting the dose response curves with a four parameter logistic equation where $\%_{inhibition} = Min_{\%inhibition} + (Max_{\%inhibition} - Min_{\%inhibition})/(1 + ([drug]/IC_{50})^{-n})$, in which $\%_{inhibition}$ represents the percentage of peak current inhibited after block by each drug, $Min_{\%inhibition}$ and $Max_{\%inhibition}$ are the minimal and maximum % block that best fit the plateaus of the curve for each drugs, [drug] is the concentration of drug, and n is the slope. The four parameters were fit with no constraints except for the tonic block of lidocaine and lacosamide (Figure 1D and 1E) for which the $Max_{\%inhibition}$ was constrained to a maximum value of 100%.

Molecular Pharmacology Fast Forward. Published on September 16, 2020 as DOI: 10.1124/molpharm.120.000048
This article has not been copyedited and formatted. The final version may differ from this version.

The apparent binding rate (K_{ON}) was measured using the time-dependent inhibition of I_{Na} during a variable length conditioning pulse. The time-dependent inhibition of I_{NaP} for each concentration was fitted with an exponential decay function having a time constant (τ). Values for 1/τ were plotted against the drug concentrations, and best fitted with a linear function. The slope represents the apparent binding rate (K_{ON}) of the drug. The apparent unbinding rate (K_{OFF}) was measured using the time-dependent delay in the recovery of I_{Na} following an inactivating conditioning pulse. The recovery time course for each drug was fit with a single exponential equation to obtain a recovery time constant, τ_{OFF}. The recovery time constant of the 3 highest concentrations used for each drug was averaged and the (K_{OFF}) was calculated using $K_{OFF} = 1/\tau_{OFF}$.

Molecular Pharmacology Fast Forward. Published on September 16, 2020 as DOI: 10.1124/molpharm.120.000048
This article has not been copyedited and formatted. The final version may differ from this version.

RESULTS

Eleclazine and GS-967 exert limited tonic block in hiPSC-derived cardiomyocytes

We previously reported that 1 μM GS-967 inhibits 18% of I_{NaP} conducted by human $Na_V1.5$ channels expressed in heterologous (tsA201) cells (Potet et al., 2016). Based on this finding we predicted that GS-967 and eleclazine would exhibit similar effects on I_{NaP} in human iPSC-derived cardiomyocytes. We performed automated patch clamp recordings of hiPSC-derived cardiomyocytes using the Syncropatch 768PE platform. Based on RNA-sequencing data performed on our hiPSC-derived cardiomyocytes, *SCN5A* ($Na_V1.5$) accounts for 84% of the expressed sodium channels (data not shown). No other functional sodium channel genes were represented more than 5%. Cardiomyocytes were held at -120 mV and currents were evoked by depolarizations to -10 mV every 5 s. This infrequent pulsing protocol reveals drug interactions with the resting or open state of the channel and minimizes the effects of UDB, thereby providing a reasonable estimate of the extent to which GS-967 and eleclazine produce I_{NaP} tonic block. In all experiments, we used the single dose method to test the compounds. As shown in Fig. 1, GS-967 or eleclazine at 1 μM exhibited limited tonic block of I_{NaP} (14 ± 2% and 6 ± 3% for GS-967 and eleclazine respectively; n = 25-27). The maximum tonic block observed for GS-967 and eleclazine was 34 ± 3% and 43 ± 7% at 10 and 100 μM, respectively (Fig. 1). Higher concentrations could not be assayed due to the limited solubility of both compounds. To study the pharmacology of I_{Na} in hiPSC-derived cardiomyocytes we recorded sodium current from more than 2500 cells (Fig. S1).

Molecular Pharmacology Fast Forward. Published on September 16, 2020 as DOI: 10.1124/molpharm.120.000048
This article has not been copyedited and formatted. The final version may differ from this version.

Figure 1 shows the concentration-response curves for I_{NaP} tonic block comparing GS-967, eleclazine, ranolazine, lidocaine and lacosamide. GS-967 and eleclazine exhibited similar IC_{50} values (1 and 2.5 μM, respectively) and had limited tonic block efficacy (Table 1). By contrast, ranolazine, lidocaine and lacosamide exerted stronger maximum tonic block (for the maximal concentration tested) but with lower potency (IC_{50} = 457, 1175 and 1241 μM, respectively). We concluded that GS-967 and eleclazine exert less tonic block of I_{NaP} in hiPSC-derived cardiomyocytes compared to ranolazine, lidocaine and lacosamide.

Use-dependent block of I_{NaP} in hiPSC-derived cardiomyocytes

We previously demonstrated that GS-967 exerts a strong UDB of $Na_V1.5$ I_{NaP} in heterologous cells with greater potency than lidocaine and ranolazine (Potet et al., 2016). Others have shown that eleclazine can also exert UDB of $Na_V1.5$ expressed in tsA201 cells (El-Bizri et al., 2018a; El-Bizri et al., 2018b; El-Bizri et al., 2018c). This motivated us to examine whether GS-967 and eleclazine exert similar effects in human cardiomyocytes.

We compared UDB by GS-967, eleclazine, ranolazine, lidocaine, and lacosamide in hiPSC-derived cardiomyocytes using two different protocols. First, we applied a series of 30 short (20 ms) depolarizing pulses (to -20 mV) at two frequencies (2 and 10 Hz). Second, we used longer (400 ms) depolarizing pulses (-20 mV) at a low frequency (2 Hz) to mimic the physiological cardiac cycle. In the absence of drugs, there was a ~4 and ~14% reduction of channel availability (frequency dependent inactivation) with the

Molecular Pharmacology Fast Forward. Published on September 16, 2020 as DOI: 10.1124/molpharm.120.000048
This article has not been copyedited and formatted. The final version may differ from this version.

short pulse protocol at 2 and 10 Hz, respectively, and a ~23% reduction with the longer pulse protocol (Fig. S2, S3 and S4). Following bath application of drugs, repetitive pulsing was associated with a progressive reduction of $Na_V1.5$ I_{NaP} consistent with UDB and frequency dependent inactivation of the channel (Fig. S2, S3 and S4). To quantify the extent of UDB, we normalized the current amplitude measured after drug exposure by the current measured before drug application (Fig. 2A). The potency of each drug at producing UDB was compared by plotting the concentration-response curves (Fig. 2B, C and D).

All drugs exhibited limited UDB at 2 Hz using the 20 ms voltage step (Fig. 2B, Fig.S2). However, at 10 Hz and at 2 Hz using the longer protocol, all drugs showed greater UDB efficacy (Fig. 2C, 2D, Fig. S3 and S4). Eleclazine and GS-967 exhibited much greater UDB potency than ranolazine, lidocaine, and lacosamide. The order of UDB potency for the 5 drugs tested was the same as that found for tonic block. The calculated IC_{50} values for UDB at 10 Hz were 0.07 μM for GS-967, 0.6 μM for eleclazine, 7.8 μM for ranolazine, 133.5 μM for lidocaine and 158.5 μM for lacosamide (Figure 2C and Table 1). At 10 Hz, eleclazine and GS-967 were 222-fold and 1907-fold more potent, respectively, than lidocaine, one of most well characterized use-dependent sodium channel blockers.

Eleclazine and GS-967 affect recovery from inactivation and exhibit moderate unbinding kinetics

To explore plausible mechanisms to explain the UDB of I_{NaP} in hiPSC-derived cardiomyocytes by GS-967 and eleclazine, we first examined recovery from slow

Molecular Pharmacology Fast Forward. Published on September 16, 2020 as DOI: 10.1124/molpharm.120.000048
This article has not been copyedited and formatted. The final version may differ from this version.

inactivation. This was done by utilizing a standard two-pulse protocol consisting of a depolarizing (-20 mV) 1000 ms pulse to reach maximum inhibition of peak I_{Na}, followed by a variable duration recovery step to -120 mV and a final test pulse (-20 mV, 20 ms) (voltage protocol illustrated in Fig. S5). Channel availability after the end of the recovery interval was normalized to initial values and plotted against the recovery time. The time course of recovery was slowed by all the drugs in a concentration-dependent manner (Fig. S5). The delayed recovery from inactivation reflects the dissociation of the drug from the channels, which can be quantified by comparing the recovery rate in the absence and presence of the compound (to remove drug-independent inactivation) (Fig.3). The unbinding rate (K_{OFF}) was then calculated by fitting the dissociation time course. The calculated K_{OFF} was 1.6 s^{-1} and 1.5 s^{-1} for GS-967 and eleclazine, respectively, which is similar to lidocaine (1.1 s^{-1}) but an order of magnitude slower than ranolazine (16.2 s^{-1}) and 4-times more rapid than lacosamide (0.4 s^{-1}) (Fig. 3).

Eleclazine and GS-967 exhibit rapid binding kinetics

Because UDB can be due to accumulation of channels in a slow inactivated state evoked by prolonged membrane depolarization, we investigated whether kinetic differences in the rate of entry into slow inactivation could account for UDB by GS-967 and eleclazine in hiPSC-cardiomyocytes. To assess the onset of slow inactivation, cells were held at -120 mV and then depolarized to -20 mV for a variable duration (2-1000 ms) followed by a brief recovery pulse (-120 mV for 20 ms) and a final 20 ms test pulse to -20 mV (voltage protocol illustrated in Fig. 4 and Fig. S6). The proportion of channels entering slow inactivation was estimated by normalizing to initial values (current

Molecular Pharmacology Fast Forward. Published on September 16, 2020 as DOI: 10.1124/molpharm.120.000048
This article has not been copyedited and formatted. The final version may differ from this version.

recorded at P1) the current obtained after the short recovery pulse (current recorded at P2) and plotted against the first pulse duration. To assess the development of inhibition, we normalized the development of slow inactivation in the absence and presence of the compound to remove drug-independent inactivation (Fig. 4A-D). We could not measure the development of inhibition for ranolazine due its short dissociation time constant (τ_{OFF} = 62 ms, Fig. 3). The brief 20 ms recovery pulse to -120 mV was long enough to allow ranolazine to apparently unbind. The time-dependent inhibition of the Na^+ currents shown in (Fig. 4A-D) was fitted with an exponential decay function having time constant τ. The $1/\tau$ values were then plotted against the drug concentrations, and best fitted with a linear function (Fig. 4E). The slope represents the apparent binding rate (K_{ON}) of the drug. As shown in Fig. 4E, the K_{ON} for GS-967, eleclazine, lidocaine and lacosamide were 25.7, 4.6, 0.2 and 0.003 $s^{-1}\mu M^{-1}$, respectively. The K_{ON} for ranolazine was estimated from the Kd value (6.5 µM; equivalent to the K_{OFF}/K_{ON} ratio). This Kd value is nearly identical to the IC_{50} value measured in the dose-response curve (Fig. 2D). The estimated K_{ON} for ranolazine was 2.5 $s^{-1}\mu M^{-1}$. Data for all 5 drugs are summarized in Fig. 5. Eleclazine and GS-967 exhibit a higher association rate compared to ranolazine, lidocaine and lacosamide, but have rapid dissociation rates similar to lidocaine. Based on this analysis, the greater UDB potency of GS-967 and eleclazine is well correlated with the higher association rates of these two compounds.

Molecular Pharmacology Fast Forward. Published on September 16, 2020 as DOI: 10.1124/molpharm.120.000048
This article has not been copyedited and formatted. The final version may differ from this version.

DISCUSSION

In this study, we used hiPSC-derived cardiomyocytes and automated patch clamp recording to elucidate the mechanism of action of two novel sodium channel blockers with demonstrated potent antiarrhythmic effects in various *in vitro* and *in vivo* models. Previously, the antiarrhythmic effects of GS-967 and eleclazine were attributed to preferential suppression of I_{NaL} (Bacic et al., 2017; Belardinelli et al., 2013; Bossu et al., 2018; Burashnikov et al., 2015; El-Bizri et al., 2018a; Fuller et al., 2016; Pezhouman et al., 2014). Here we offer evidence for other potentially important biophysical effects of GS-967 and eleclazine on sodium channels in human cardiomyocytes. We specifically demonstrated that GS-967 and eleclazine exert strong effects on slow inactivation and recovery from inactivation resulting in a substantial UDB similar to class 1-b antiarrhythmic drugs. These revelations may help explain the pharmacological effects of GS-967 and eleclazine in arrhythmia models.

A novel feature of our study is the use of automated planar patch clamp recording of hiPSC-derived cardiomyocytes in a 384-well configuration. While the use of planar patch clamp to record Na^+ current in hiPSC-derived cardiomyocytes was described previously (Li et al., 2019; Rajamohan et al., 2016), these reports used much lower throughput platforms capable of recording from only 4-8 cells at a time. Our use of the 384-well platform in our study enabled a more robust capability to examine the pharmacological actions of multiple drugs simultaneously. The higher throughput also allowed us to use test single drug concentrations per well, and to measure binding and unbinding kinetics for 5 different drugs. These data demonstrate the feasibility of

Molecular Pharmacology Fast Forward. Published on September 16, 2020 as DOI: 10.1124/molpharm.120.000048
This article has not been copyedited and formatted. The final version may differ from this version.

studying the pharmacological actions of drugs on the native human cardiac sodium current in hiPSC-derived cardiomyocytes.

Unique to our study, we demonstrated that GS-967 and eleclazine exert potent UDB of I_{NaP} in hiPSC-derived cardiomyocytes. Previously, UDB of GS-967 and eleclazine has not been examined in hiPSC-derived cardiomyocytes (Alves Bento et al., 2015; Belardinelli et al., 2013; Bonatti et al., 2014; Burashnikov et al., 2015; Carneiro et al., 2015; El-Bizri et al., 2018a; Fuller et al., 2016; Portero et al., 2017). Among the sodium channel blockers we tested, GS-967 exhibited the greatest UDB potency with IC_{50} values ranging from 50 to 90 nM depending on stimulation frequency and duration of the voltage steps (Fig. 2). GS-967 and eleclazine exerted UDB that was qualitatively similar to lidocaine (a prototypic use-dependent blocker of sodium channels) but with a greater potency. The greater UDB potency was correlated with the unique on and off rate kinetics for these novel sodium channel blockers. By contrast, the rapid dissociation of ranolazine (K_{OFF}, Fig. 3 and 5) and the slow binding kinetics of lacosamide (K_{ON}, Fig. 4 and 5) were both correlated with less potent UDB.

GS-967 and eleclazine were originally demonstrated to exert potent antiarrhythmic effects in rabbit ventricular, canine and pig myocytes/heart by a proposed mechanism of action involving preferential I_{NaL} block (Bacic et al., 2017; Belardinelli et al., 2013; Fuller et al., 2016; Sicouri et al., 2013). In a more recent study, despite completely abolishing dofetilide-induced torsades de pointes (TdP) in a chronic atrioventricular block dog model, GS-967 did not completely suppress early afterdepolarizations (EADs) (Bossu et

Molecular Pharmacology Fast Forward. Published on September 16, 2020 as DOI: 10.1124/molpharm.120.000048
This article has not been copyedited and formatted. The final version may differ from this version.

al., 2018). The authors concluded that GS-967 predominantly affects the perpetuation, but not the initiation, of arrhythmic events into TdP and that I_{NaL} density does not play a critical role in the moderate *in vitro* antiarrhythmic effect. Because the GS-967 and eleclazine concentrations used in those studies range from 0.2-1 μM, a range sufficient to suppress I_{NaL} and also to evoke UDB, we speculate that antiarrhythmic effects of these compounds may be due to the combination of I_{NaL} suppression and UDB preventing the perpetuation of the arrhythmia.

The effects of GS-967 and eleclazine resemble the effects of lidocaine, a class-Ib antiarrhythmic drug (Fig. 2). Effective class I antiarrhythmic drugs exhibit a greater efficacy in situations associated with rapid repetitive firing of action potentials (UDB) or prolonged tissue depolarization. Thus, effective arrhythmia suppression depends on the properties of the drug molecule that convey high affinity binding to the receptor on the channel pore when the channel is in the open or inactivated state. Such high affinity binding results in a slowed recovery of the drug-bound channel from inactivation as the cell membrane repolarizes (Ragsdale et al., 1996). In this study, we show that GS-967 and eleclazine, in hiPSC-derived cardiomyocytes, have very high association rates and moderate residence time comparable to lidocaine (Fig. 5). The moderate unbinding kinetics observed for GS-967 and eleclazine would limit peak I_{Na} inhibition and maintain the conduction velocity (Rajamani et al., 2016). The rapid binding of GS-967 and eleclazine would promote inhibition of late I_{Na} during phase 2 and 3 of the action potential and exert an antiarrhythmic action in the context of LQT3 syndrome (El-Bizri et

Molecular Pharmacology Fast Forward. Published on September 16, 2020 as DOI: 10.1124/molpharm.120.000048
This article has not been copyedited and formatted. The final version may differ from this version.

al., 2018c). This was the rationale for clinical trials of eleclazine for type 3 LQTS (Gilead, 2000-2015).

In conclusion, we demonstrated the feasibility of using high throughput automated patch clamp recording to examine block of cardiac sodium current by multiple drugs in hiPSC-derived cardiomyocytes. We also demonstrated that GS-967 and eleclazine are more potent use-dependent blockers of cardiomyocyte sodium current than the antiarrhythmic drugs lidocaine and ranolazine or the antiepileptic drug lacosamide. We propose that potent UDB contributes to the antiarrhythmic effects of GS-967 and eleclazine.

Molecular Pharmacology Fast Forward. Published on September 16, 2020 as DOI: 10.1124/molpharm.120.000048
This article has not been copyedited and formatted. The final version may differ from this version.

ACKNOWLEDGMENTS

The authors thank Hui-Hsuan Kuo for her technical assistance.

AUTHORSHIP CONTRIBUTIONS

Participated in research design: Potet and George.

Conducted experiments: Potet and Egecioglu.

Performed data analysis: Potet.

Wrote or contributed to the writing of the manuscript: Potet, Burridge, and George.

REFERENCES

Alves Bento AS, Bacic D, Saran Carneiro J, Nearing BD, Fuller H, Justo FA, Rajamani S, Belardinelli L and Verrier RL (2015) Selective late I_{Na} inhibition by GS-458967 exerts parallel suppression of catecholamine-induced hemodynamically significant ventricular tachycardia and T-wave alternans in an intact porcine model. *Heart Rhythm* **12**(12): 2508-2514.

Antzelevitch C, Nesterenko V, Shryock JC, Rajamani S, Song Y and Belardinelli L (2014) The role of late I_{Na} in development of cardiac arrhythmias. *Handbook of Experimental Pharmacology* **221**: 137-168.

Bacic D, Carneiro JS, Bento AA, Nearing BD, Rajamani S, Belardinelli L and Verrier RL (2017) Eleclazine, an inhibitor of the cardiac late sodium current, is superior to flecainide in suppressing catecholamine-induced ventricular tachycardia and T-wave alternans in an intact porcine model. *Heart Rhythm* **14**(3): 448-454.

Belardinelli L, Liu G, Smith-Maxwell C, Wang WQ, El-Bizri N, Hirakawa R, Karpinski S, Li CH, Hu L, Li XJ, Crumb W, Wu L, Koltun D, Zablocki J, Yao L, Dhalla AK, Rajamani S and Shryock JC (2013) A novel, potent, and selective inhibitor of cardiac late sodium current suppresses experimental arrhythmias. *J Pharmacol Exp Ther* **344**(1): 23-32.

Bennett PB, Yazawa K, Makita N and George AL, Jr. (1995) Molecular mechanism for an inherited cardiac arrhythmia. *Nature* **376**(6542): 683-685.

Bonatti R, Silva AF, Batatinha JA, Sobrado LF, Machado AD, Varone BB, Nearing BD, Belardinelli L and Verrier RL (2014) Selective late sodium current blockade with GS-458967 markedly reduces ischemia-induced atrial and ventricular repolarization alternans and ECG heterogeneity. *Heart Rhythm* **11**(10): 1827-1835.

Bossu A, Houtman MJC, Meijborg VMF, Varkevisser R, Beekman HDM, Dunnink A, de Bakker JMT, Mollova N, Rajamani S, Belardinelli L, van der Heyden MAG and Vos MA (2018) Selective late sodium current inhibitor GS-458967 suppresses Torsades de

Pointes by mostly affecting perpetuation but not initiation of the arrhythmia. *Br J Pharmacol* **175**(12): 2470-2482.

Burashnikov A, Di Diego JM, Goodrow RJ, Jr., Belardinelli L and Antzelevitch C (2015) Atria are more sensitive than ventricles to GS-458967-induced inhibition of late sodium current. *J Cardiovasc Pharmacol Ther* **20**(5): 501-508.

Burridge PW, Holmstrom A and Wu JC (2015) Chemically defined culture and cardiomyocyte differentiation of human pluripotent stem cells. *Curr Protoc Hum Genet* **87**: 21 23 21-21 23 15.

Burridge PW, Li YF, Matsa E, Wu H, Ong SG, Sharma A, Holmstrom A, Chang AC, Coronado MJ, Ebert AD, Knowles JW, Telli ML, Witteles RM, Blau HM, Bernstein D, Altman RB and Wu JC (2016) Human induced pluripotent stem cell-derived cardiomyocytes recapitulate the predilection of breast cancer patients to doxorubicin-induced cardiotoxicity. *Nat Med* **22**(5): 547-556.

Burridge PW, Matsa E, Shukla P, Lin ZC, Churko JM, Ebert AD, Lan F, Diecke S, Huber B, Mordwinkin NM, Plews JR, Abilez OJ, Cui B, Gold JD and Wu JC (2014) Chemically defined generation of human cardiomyocytes. *Nat Methods* **11**(8): 855-860.

Carneiro JS, Bento AS, Bacic D, Nearing BD, Rajamani S, Belardinelli L and Verrier RL (2015) The selective cardiac late sodium current inhibitor GS-458967 suppresses autonomically triggered atrial fibrillation in an intact porcine model. *J Cardiovasc Electrophysiol* **26**(12): 1364-1369.

El-Bizri N, Li CH, Liu GX, Rajamani S and Belardinelli L (2018a) Selective inhibition of physiological late Na^+ current stabilizes ventricular repolarization. *Am J Physiol Heart Circ Physiol* **314**(2): H236-H245.

El-Bizri N, Xie C, Liu L, Limberis J, Krause M, Hirakawa R, Nguyen S, Tabuena DR, Belardinelli L and Kahlig KM (2018b) Eleclazine exhibits enhanced selectivity for long QT syndrome type 3-associated late Na^+ current. *Heart Rhythm* **15**(2): 277-286.

El-Bizri N, Xie C, Liu L, Limberis J, Krause M, Hirakawa R, Nguyen S, Tabuena DR, Belardinelli L and Kahlig KM (2018c) Eleclazine exhibits enhanced selectivity for long QT syndrome type 3-associated late Na^+ current. *Heart Rhythm* **15**(2): 277-286.

Errington AC, Stohr T, Heers C and Lees G (2008) The investigational anticonvulsant lacosamide selectively enhances slow inactivation of voltage-gated sodium channels. *Mol Pharmacol* **73**(1): 157-169.

Fuller H, Justo F, Nearing BD, Kahlig KM, Rajamani S, Belardinelli L and Verrier RL (2016) Eleclazine, a new selective cardiac late sodium current inhibitor, confers concurrent protection against autonomically induced atrial premature beats, repolarization alternans and heterogeneity, and atrial fibrillation in an intact porcine model. *Heart Rhythm* **13**(8): 1679-1686.

Gilead (2000-2015) Gilead Sciences: Effect of eleclazine on shortening of the QT interval, safety, and tolerability in adults with long QT syndrome type 3. *In: ClinicalTrialsgov [Internet] Bethesda (MD): National Library of Medicine (US)*: Available from https://clinicaltrials.gov/show/NCT02300558 NLM identifier: NCT02300558.

Gupta T, Khera S, Kolte D, Aronow WS and Iwai S (2015) Antiarrhythmic properties of ranolazine: A review of the current evidence. *Int J Cardiol* **187**: 66-74.

Herzog RI, Liu C, Waxman SG and Cummins TR (2003) Calmodulin binds to the C terminus of sodium channels $Na_V1.4$ and $Na_V1.6$ and differentially modulates their functional properties. *J Neurosci* **23**(23): 8261-8270.

Hodgkin AL and Huxley AF (1952) A quantitative description of membrane current and its application to conduction and excitation in nerve. *J Physiol* **117**(4): 500-544.

Kahlig KM, Hirakawa R, Liu L, George AL, Jr., Belardinelli L and Rajamani S (2014) Ranolazine reduces neuronal excitability by interacting with inactivated states of brain sodium channels. *Mol Pharmacol* **85**(1): 162-174.

Koltun DO, Parkhill EQ, Elzein E, Kobayashi T, Notte GT, Kalla R, Jiang RH, Li X, Perry TD, Avila B, Wang WQ, Smith-Maxwell C, Dhalla AK, Rajamani S, Stafford B, Tang J,

Mollova N, Belardinelli L and Zablocki JA (2016) Discovery of triazolopyridine GS-458967, a late sodium current inhibitor (Late $I_{Na}i$) of the cardiac $Na_V1.5$ channel with improved efficacy and potency relative to ranolazine. *Bioorg Med Chem Lett* **26**(13): 3202-3206.

Le Grand B, Vie B, Talmant JM, Coraboeuf E and John GW (1995) Alleviation of contractile dysfunction in ischemic hearts by slowly inactivating Na^+ current blockers. *Am J Physiol* **269**(2 Pt 2): H533-540.

Li W, Luo X, Ulbricht Y, Wagner M, Piorkowski C, El-Armouche A and Guan K (2019) Establishment of an automated patch-clamp platform for electrophysiological and pharmacological evaluation of hiPSC-CMs. *Stem Cell Res* **41**: 101662.

Pezhouman A, Madahian S, Stepanyan H, Ghukasyan H, Qu Z, Belardinelli L and Karagueuzian HS (2014) Selective inhibition of late sodium current suppresses ventricular tachycardia and fibrillation in intact rat hearts. *Heart Rhythm* **11**(3): 492-501.

Pignier C, Rougier JS, Vie B, Culie C, Verscheure Y, Vacher B, Abriel H and Le Grand B (2010) Selective inhibition of persistent sodium current by F 15845 prevents ischaemia-induced arrhythmias. *Br J Pharmacol* **161**(1): 79-91.

Portero V, Casini S, Hoekstra M, Verkerk AO, Mengarelli I, Belardinelli L, Rajamani S, Wilde AAM, Bezzina CR, Veldkamp MW and Remme CA (2017) Anti-arrhythmic potential of the late sodium current inhibitor GS-458967 in murine Scn5a-1798insD$^{+/-}$ and human SCN5A-1795insD$^{+/-}$ iPSC-derived cardiomyocytes. *Cardiovasc Res* **113**(7): 829-838.

Potet F, Vanoye CG and George AL, Jr. (2016) Use-dependent block of human cardiac sodium channels by GS967. *Mol Pharmacol* **90**(1): 52-60.

Ragsdale DS, McPhee JC, Scheuer T and Catterall WA (1996) Common molecular determinants of local anesthetic, antiarrhythmic, and anticonvulsant block of voltage-gated Na^+ channels. *Proc Natl Acad Sci U S A* **93**(17): 9270-9275.

Rajamani S, Liu G, El-Bizri N, Guo D, Li C, Chen XL, Kahlig KM, Mollova N, Elzein E, Zablocki J and Belardinelli L (2016) The novel late Na^+ current inhibitor, GS-6615 (eleclazine) and its anti-arrhythmic effects in rabbit isolated heart preparations. *Br J Pharmacol* **173**(21): 3088-3098.

Rajamohan D, Kalra S, Duc Hoang M, George V, Staniforth A, Russell H, Yang X and Denning C (2016) Automated electrophysiological and pharmacological evaluation of human pluripotent stem cell-derived cardiomyocytes. *Stem Cells Dev* **25**(6): 439-452.

Ruan Y, Liu N and Priori SG (2009) Sodium channel mutations and arrhythmias. *Nature reviews Cardiology* **6**(5): 337-348.

Sicouri S, Belardinelli L and Antzelevitch C (2013) Antiarrhythmic effects of the highly selective late sodium channel current blocker GS-458967. *Heart Rhythm* **10**(7): 1036-1043.

Song Y, Shryock JC, Wagner S, Maier LS and Belardinelli L (2006) Blocking late sodium current reduces hydrogen peroxide-induced arrhythmogenic activity and contractile dysfunction. *J Pharmacol Exp Ther* **318**(1): 214-222.

Strichartz G, Rando T and Wang GK (1987) An integrated view of the molecular toxinology of sodium channel gating in excitable cells. *Annu Rev Neurosci* **10**: 237-267.

Szel T, Koncz I, Jost N, Baczko I, Husti Z, Virag L, Bussek A, Wettwer E, Ravens U, Papp JG and Varro A (2011) Class I/B antiarrhythmic property of ranolazine, a novel antianginal agent, in dog and human cardiac preparations. *Eur J Pharmacol* **662**(1-3): 31-39.

FOOTNOTES

This work was funded in part by a grant from Fondation Leducq and through research investments by the Northwestern Medicine Catalyst Fund.

Molecular Pharmacology Fast Forward. Published on September 16, 2020 as DOI: 10.1124/molpharm.120.000048
This article has not been copyedited and formatted. The final version may differ from this version.

DISCLOSURES

Dr. Potet is a paid consultant for Praxis Precision Medicines, Inc. Dr. George serves on a scientific advisory board for Amgen, Inc. and received previous grant support from Merck and Co., Gilead Sciences, Inc., and Praxis Precision Medicines, Inc.

Molecular Pharmacology Fast Forward. Published on September 16, 2020 as DOI: 10.1124/molpharm.120.000048
This article has not been copyedited and formatted. The final version may differ from this version.

LEGENDS FOR FIGURES

Figure 1. I_{NaP} tonic block in hiPSC-derived cardiomyocytes.

Top: Drug chemical structures. Middle: representative I_{NaP} traces in absence (black) and presence (red) of the drug. Bottom: I_{NaP} concentration-response curve for GS-967 (**A**), eleclazine (**B**), ranolazine (**C**), lidocaine (**D**) and lacosamide (**E**). Currents were recorded from hiPSC-derived cardiomyocytes using automated patch clamp. Human iPSC-cardiomyocytes were held at a membrane potential of -120 mV and depolarized every 5 seconds to -10 mV for 200 ms (see inset). I_{NaP} was measured at -10 mV before drug and were measured again 5 min after addition of the drug. The data are shown as a percentage of I_{NaP} normalized to the maximum current in the absence of drug (I/I_{max}). The representative current traces shown for the blocking effects of GS-967, eleclazine, ranolazine, lidocaine and lacosamide on I_{NaP} 5 min after perfusion were chosen at a concentration giving the maximum tonic block. The curves described by the solid lines were fitted by a four-parameter logistic equation. Each data symbol in the concentration response curves represent mean ± SD for n = 7-67 cells. Estimated IC_{50} values are indicated for each concentration-response curve. The 95% confidence intervals (95% CI) and Hill coefficients are provided in Table 1.

Figure 2. Concentration-response of I_{NaP} use-dependent block in hiPSC-derived cardiomyocytes by GS-967, eleclazine, ranolazine, lidocaine and lacosamide.

A, To examine use-dependent block, hiPSC-derived cardiomyocytes were held at -120 mV and pulsed to -20 mV for 400 ms at 2 Hz, with an inter-pulse potential of -120 mV (see inset). The peak currents elicited by each pulse were normalized to the peak

Molecular Pharmacology Fast Forward. Published on September 16, 2020 as DOI: 10.1124/molpharm.120.000048
This article has not been copyedited and formatted. The final version may differ from this version.

current of first pulse and plotted against the pulse number. The ratio after/before drug was plotted to assess the potency of pure UDB. GS-967: concentrations from 0.0001 to 10 μM; n = 35-67. Eleclazine: concentrations from 0.0001 to 100 μM; n = 16-29. Ranolazine concentrations from 0.01 to 100 μM; n = 23-33. Lidocaine concentrations from 0.1 to 2000 μM; n = 6-27. Lacosamide concentrations from 0.001 to 1000 μM; n = 41-145. Concentration-response relationships for use-dependent block was studied using a series of 30 short (20 ms) depolarizing pulses (-20 mV) at two different frequencies (2 and 10 Hz) or longer physiological (400 ms) depolarizing pulses (-20 mV) at a low frequency (2 Hz). The % inhibition at the 30th pulse was calculated and plotted as a function of drug concentration. **B,** Concentration-response relationships for the use-dependent block at 2 Hz using a 20 ms step. IC_{50} = 0.09, 0.9, 8.1, 156.6 and 249.5 μM for GS-967, eleclazine, ranolazine, lidocaine and lacosamide respectively. **C,** Concentration-response for use-dependent block at 10 Hz using a 20 ms step. IC_{50} = 0.07, 0.6, 7.8, 133.5 and 158.5 μM for GS-967, eleclazine, ranolazine, lidocaine and lacosamide respectively. **D,** Concentration-response for use-dependent block at 2 Hz using a 400 ms step. IC_{50} = 0.05, 0.4, 6.5, 32.6 and 40.6 μM for GS-967, eleclazine, ranolazine, lidocaine and lacosamide respectively. Data are presented as mean ± SEM in panel A for clarity, and mean ± SD in panels B, C and D. The 95% CI and Hill coefficients are provided in Table 1. The curves described by the solid lines were fitted by a four-parameter logistic equation.

Molecular Pharmacology Fast Forward. Published on September 16, 2020 as DOI: 10.1124/molpharm.120.000048
This article has not been copyedited and formatted. The final version may differ from this version.

Figure 3. Recovery from inhibition in hiPSC-derived cardiomyocytes by GS-967, eleclazine, ranolazine, lidocaine and lacosamide.

Recovery from inactivation was studied in hiPSC-derived cardiomyocytes with a standard two-pulse protocol consisting of a depolarizing (-20 mV) 1000 ms pulse to engage slow inactivation, followed by a variable duration recovery step to -120 mV and a final test pulse (-20 mV, 20 ms); see inset. Available current at the end of the recovery interval was normalized to initial values and plotted against the recovery time. To calculate the unbinding rate (K_{OFF}), the recovery of drug-bound channels was distinguished from non-bound channels by the ratio $(I_{DRUG\_REC}/I_{DRUG\_MAX})/(I_{CTR\_REC}/I_{CTR\_MAX})$, where I_{X_REC} is the proportion of channels recovered in the presence or absence of a drug and I_{X_MAX} is the maximum current obtained in the presence or absence of drug (El-Bizri et al., 2018a). The recovery time course was fit with a single exponential equation to obtain a recovery time constant, τ_{OFF}, The exponential curves appear sigmoidal because they were plotted on a log axis. The recovery time constant was averaged for each drug and the (K_{OFF}) was calculated using $K_{OFF} = 1/\tau_{OFF}$: **A**, GS-967: K_{OFF} = 1.58 s^{-1}; n = 12-32. **B,** eleclazine: K_{OFF} = 1.48 s^{-1}; n = 23-24. **C,** ranolazine: K_{OFF} = 16.2 s^{-1}; n = 16-19. **D**, lidocaine: K_{OFF} = 1.1 s^{-1}; n = 3-10. **E,** lacosamide: K_{OFF} = 0.4 s^{-1}; n = 73-127. Data represent mean ± SEM for clarity.

Figure 4. The apparent inhibition rate (K_{ON}) of GS-967 and eleclazine is more rapid than ranolazine, lidocaine and lacosamide.

The onset of slow inactivation induced by GS-967, eleclazine, ranolazine, lidocaine and lacosamide were determined in hiPSC-derived cardiomyocytes using the two-pulse

Molecular Pharmacology Fast Forward. Published on September 16, 2020 as DOI: 10.1124/molpharm.120.000048
This article has not been copyedited and formatted. The final version may differ from this version.

protocol illustrated in the inset. Concentration-response curves were plotted using the data collected after a pre-pulse of 1000 ms. The development of slow inactivation in the presence of compounds was normalized by the values determined in the absence of the compound to remove drug-independent inactivation. The time-dependent inhibition of I_{NaP} shown for eleclazine (**A**), GS-967 (**B**), lidocaine (**C**), lacosamide (**D**) was fitted by an exponential decay function with a time constant (τ). The exponential curves appear sigmoidal because they were plotted on a log axis. **E**, Values for 1/τ were plotted against the drug concentrations, and best fitted by a linear function. The slope represents the apparent binding rate (K_{ON}) of the drug. K_{ON} values for GS-967, eleclazine, lidocaine and lacosamide were 25.7, 4.6, 0.2 and 0.003 $s^{-1}\mu M^{-1}$, respectively. Data are presented as mean ± SEM for clarity.

Figure 5. Relationship between K_{ON} and K_{OFF} for GS-967, eleclazine, ranolazine, lidocaine and lacosamide in hiPSC-derived cardiomyocytes.

Relationship between the measured binding rate (K_{ON}) and the measured unbinding rate (K_{OFF}) for GS-967, eleclazine, lidocaine and lacosamide in hiPSC-derived cardiomyocytes. The K_{ON} for ranolazine was estimated as 6.5 $s^{-1}\mu M^{-1}$ from $K_d = K_{OFF}/K_{ON}$. This Kd value is nearly identical to the IC_{50} value measured in the dose-response curve (Fig. 2D). The horizontal error bars represent the standard deviation for K_{OFF}. Confidence intervals for K_{ON} are smaller than the data symbols except for lacosamide.

Molecular Pharmacology Fast Forward. Published on September 16, 2020 as DOI: 10.1124/molpharm.120.000048
This article has not been copyedited and formatted. The final version may differ from this version.

Table1. Compiled IC_{50} values and Hill coefficients for GS-967, eleclazine, ranolazine, lidocaine and lacosamide for tonic block and UDB in hiPSC-derived cardiomyocytes.

	GS-967	Eleclazine	Ranolazine	Lidocaine	Lacosamide
Tonic Block					
IC_{50} (μM)	1	2.5	457.8	1175	1241
95% CI (μM)*	0.47 - 1119	0.5 - 5.4	99.7 - 1100	826 - 1710	1070 - 1486
Hill coefficient	1	1.3	0.7	3.6	0.9
UDB 2 Hz					
IC_{50} (μM)	0.09	0.9	8.1	156.6	249.5
95% CI (μM)	0.07 - 0.12	0.16 - 6.31	6.5 - 10.7	83.8 - 453.5	158.4 - 876.6
Hill coefficient	2.8	1.2	1.9	1.4	1
UDB 10 Hz					
IC_{50} (μM)	0.07	0.6	7.8	133.5	158.5
95% CI (μM)	0.06 - 0.08	0.28 - 1007	6.7 - 9.1	63.9 - 1161	131.4 - 212.9
Hill coefficient	1.8	1	2.8	0.7	1.2
UDB 2 Hz (400 ms)					
IC_{50} (μM)	0.05	0.4	6.5	32.6	40.6
95% CI (μM)	0.04 - 0.06	0.28 - 0.57	5.1 - 8.2	23.1 - 49	31.8 - 51.1
Hill coefficient	2.6	1.8	2.7	1.1	1.3

*The confidence intervals for IC_{50} values were calculated using the asymmetrical (likelihood) method and determined from one fit of the pooled data.

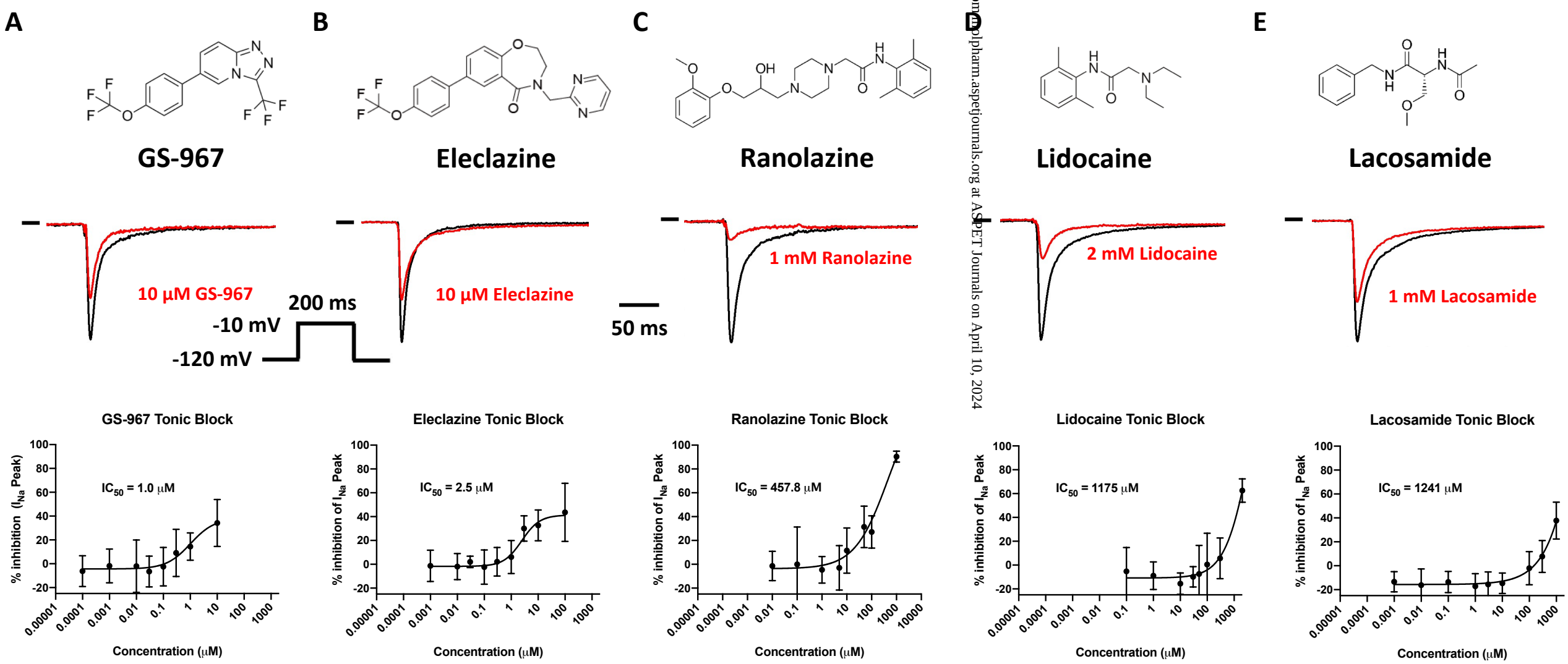

Figure 1

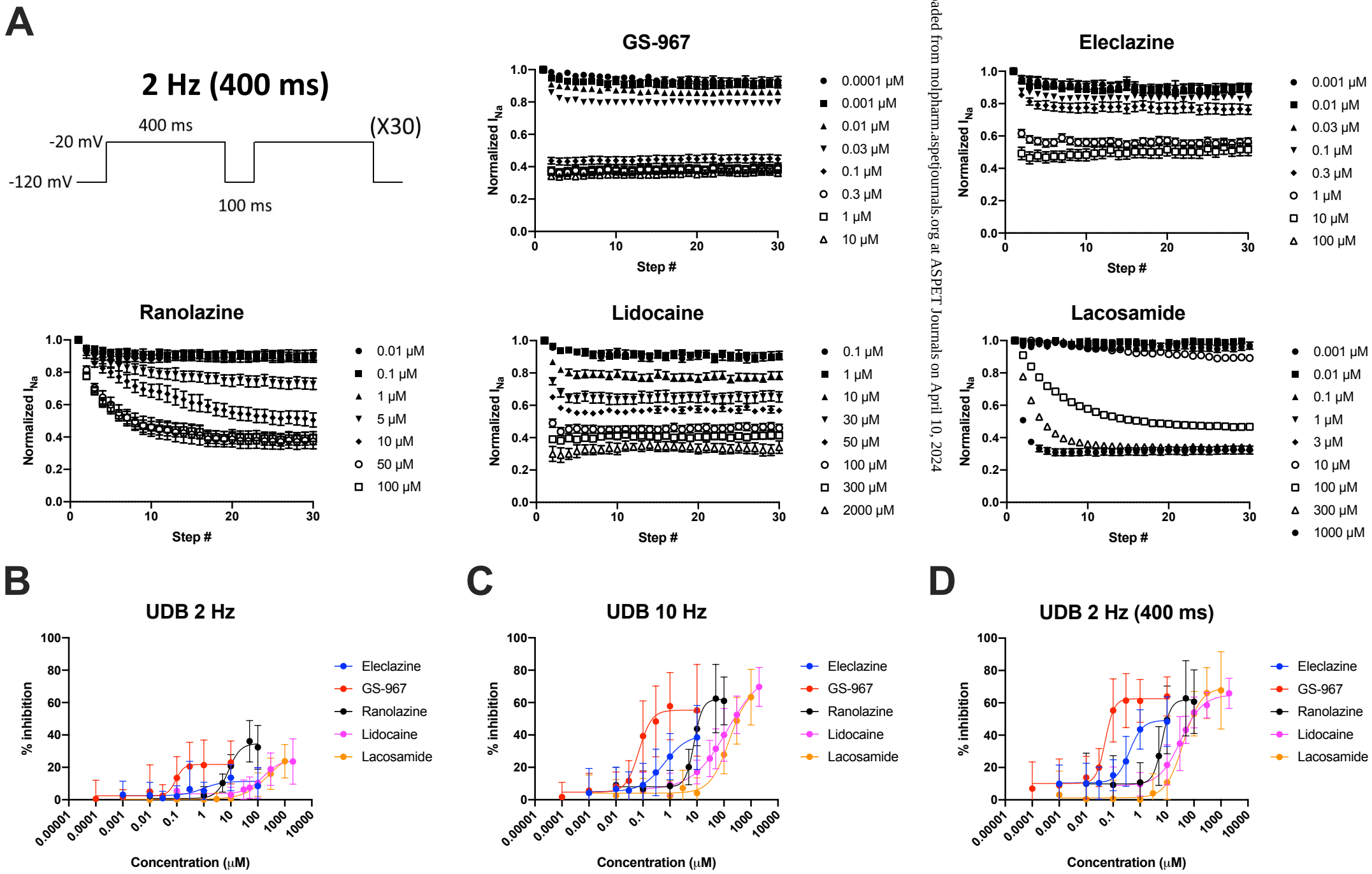

Figure 2

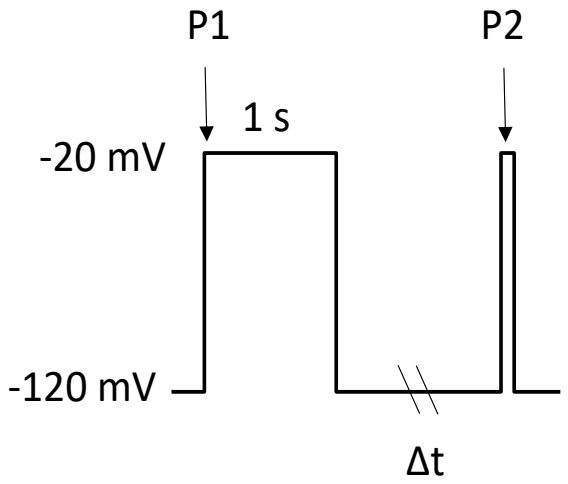

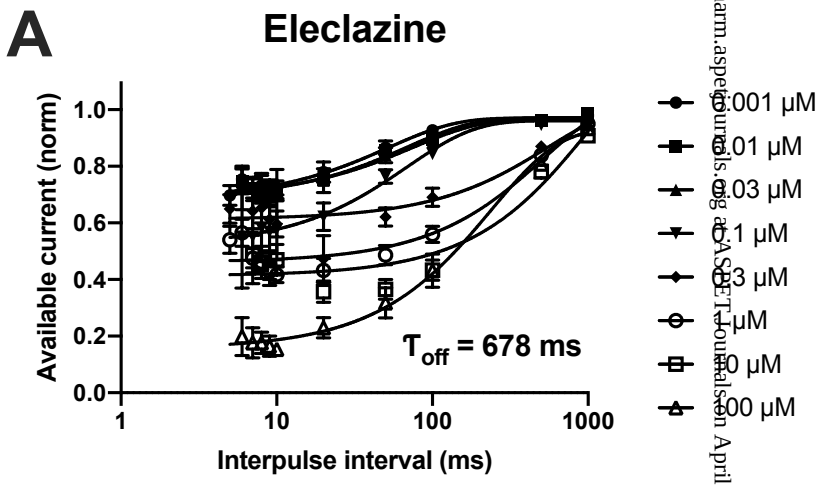

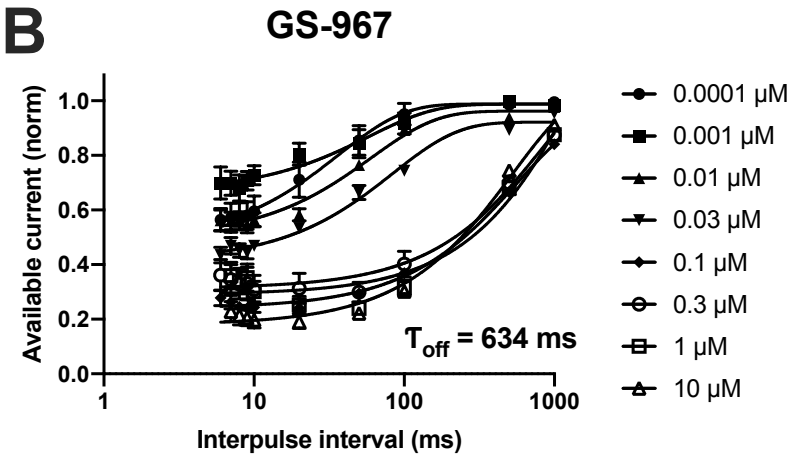

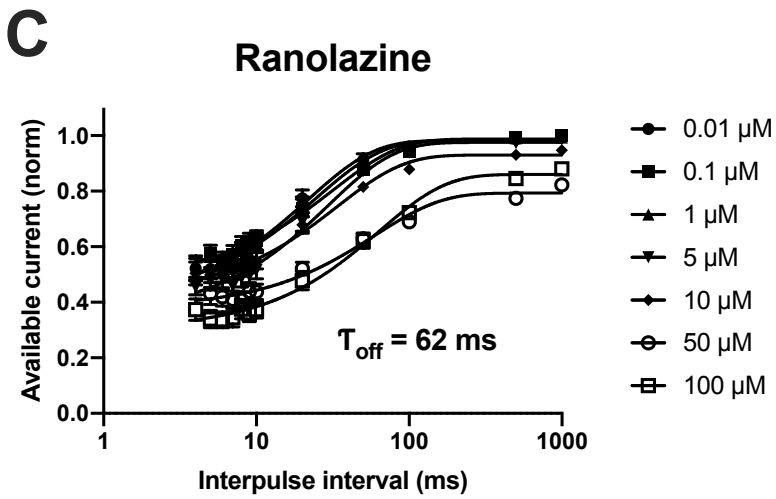

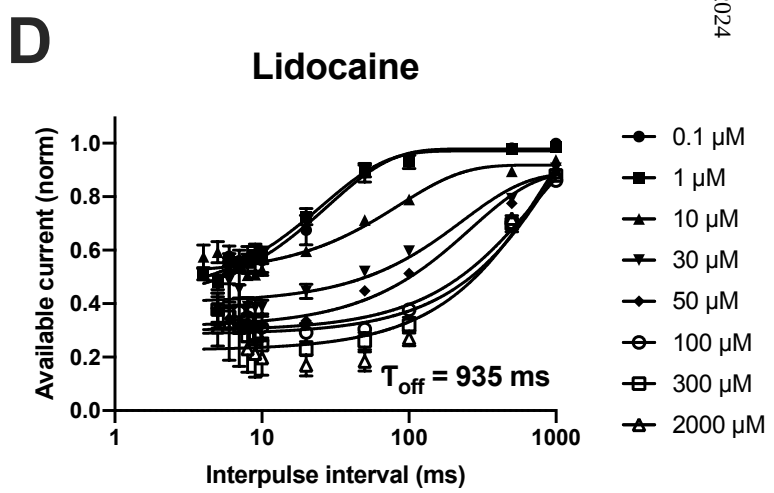

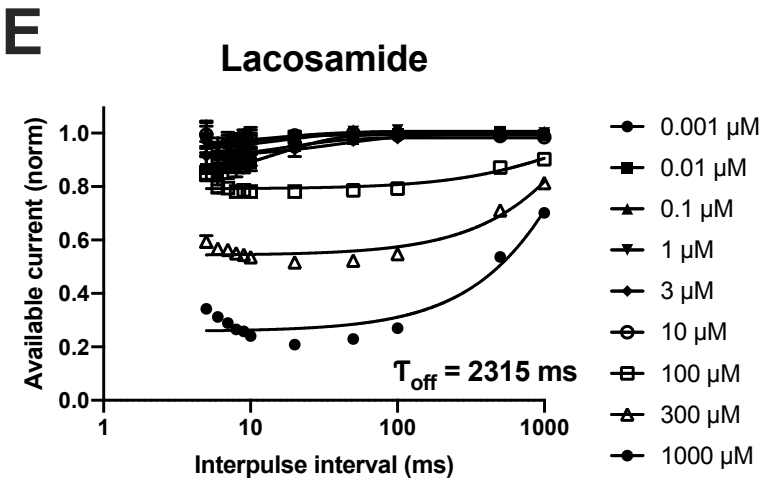

Figure 3

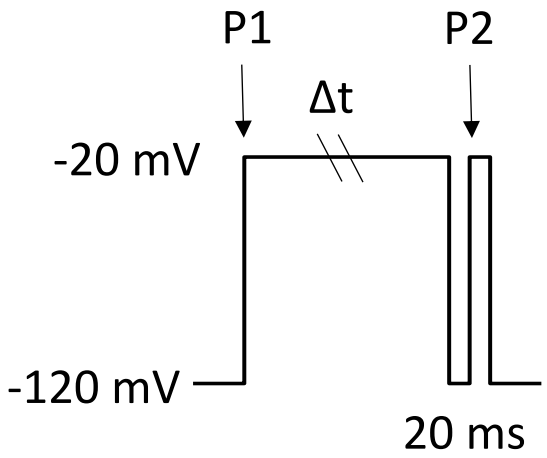

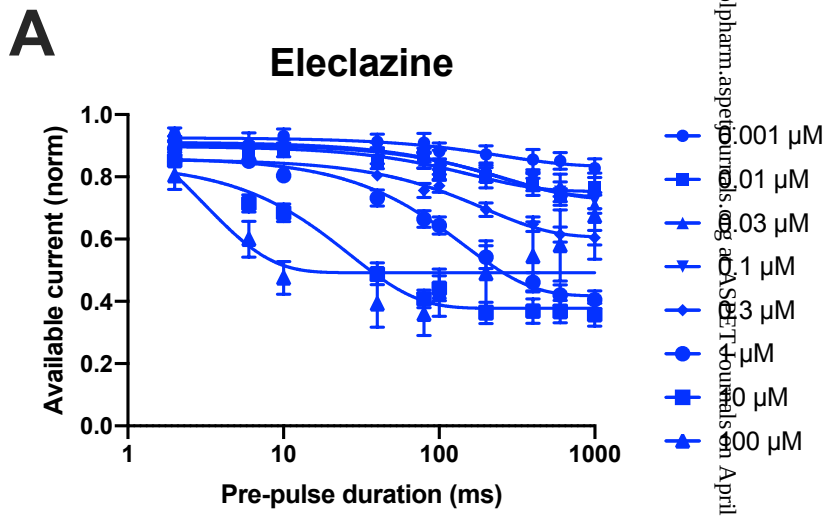

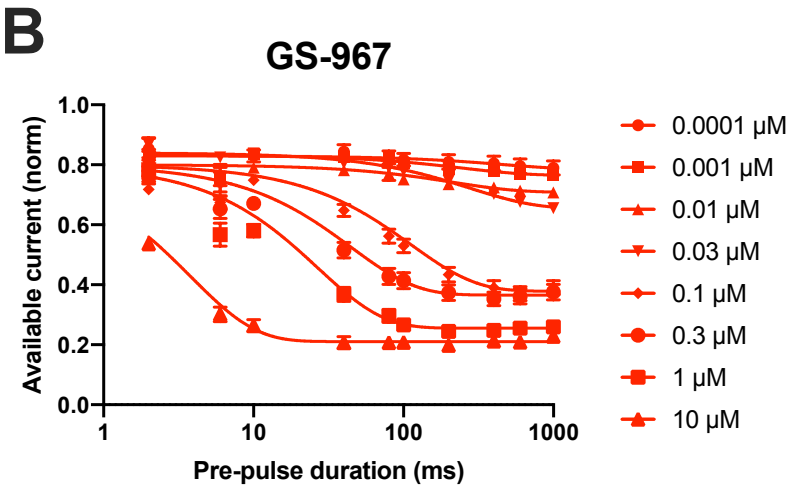

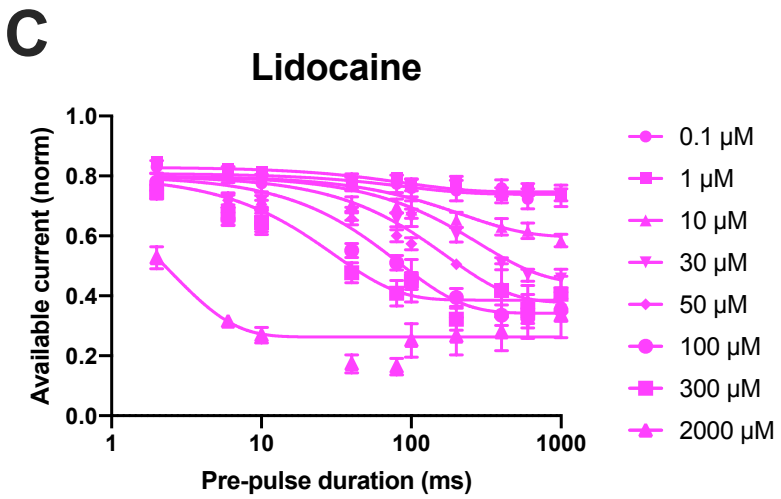

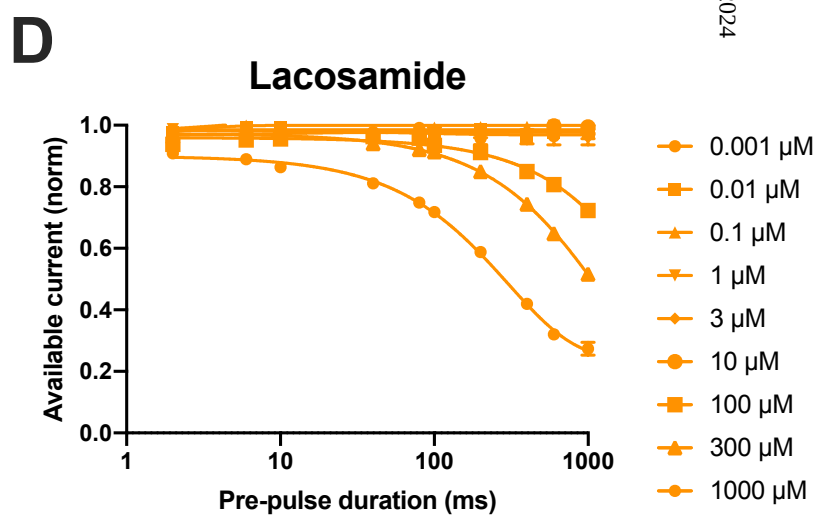

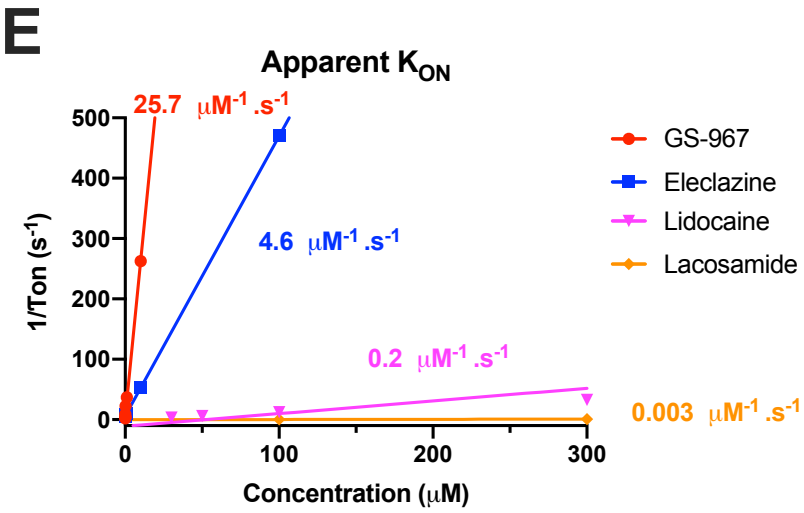

Figure 4

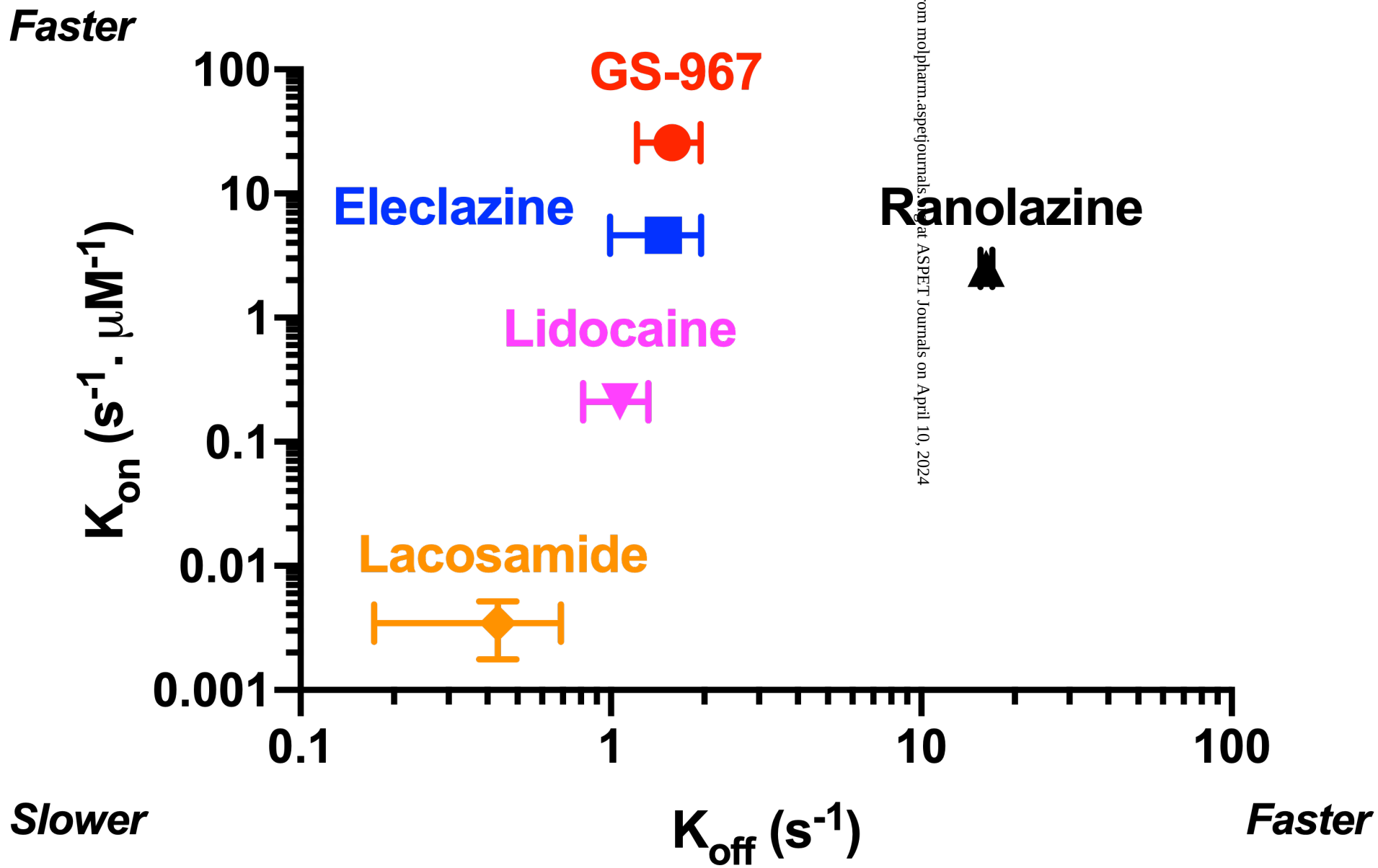

Figure 5

SUPPLEMENTAL MATERIAL

GS-967 and Eleclazine Block Sodium Channels in Human Induced Pluripotent Stem Cell-derived Cardiomyocytes

Franck Potet, Defne Emel Egecioglu, Paul W. Burridge and Alfred L. George, Jr.

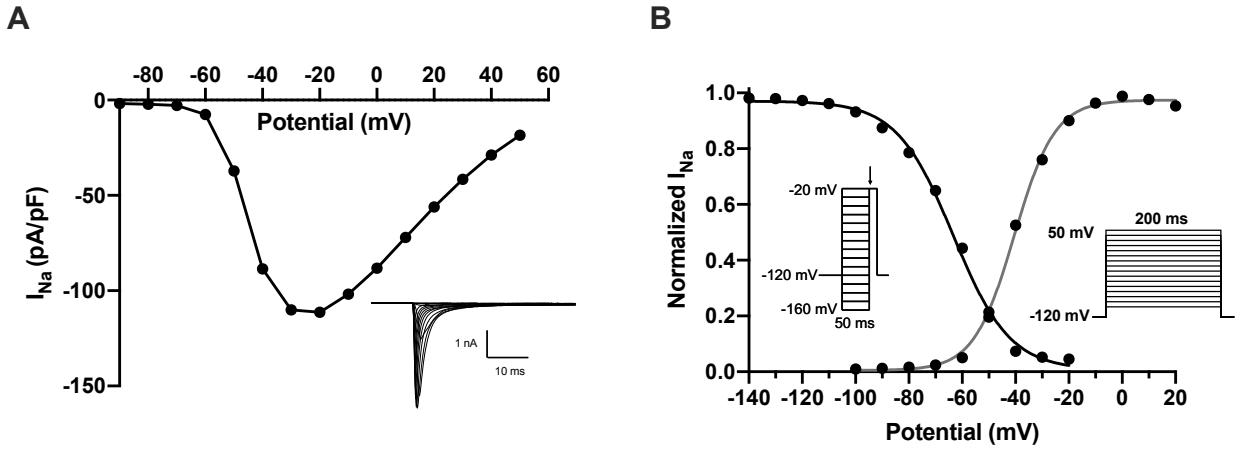

Fig. S1. Biophysical properties of I_{Na} in human iPSC-derived cardiomyocytes.
A, averaged current-voltage relationship of I_{Na} from hiPSC-derived cardiomyocytes (inset: averaged current traces). **B,** I_{Na} voltage dependence of activation and inactivation in hiPSC-derived cardiomyocytes. Inset: voltage protocols used to assess voltage dependence of activation and inactivation. The half maximum voltage for inactivation was $V_{0.5}$ = -23.6 ± 0.1 mV (n = 2686). The half maximum voltage for activation was $V_{0.5}$ = -39.4 ± 0.2 mV (n = 1600). $V_{0.5}$ were determined by using the Boltzmann equation. All data are presented as mean ± SEM.

SUPPLEMENTAL MATERIAL

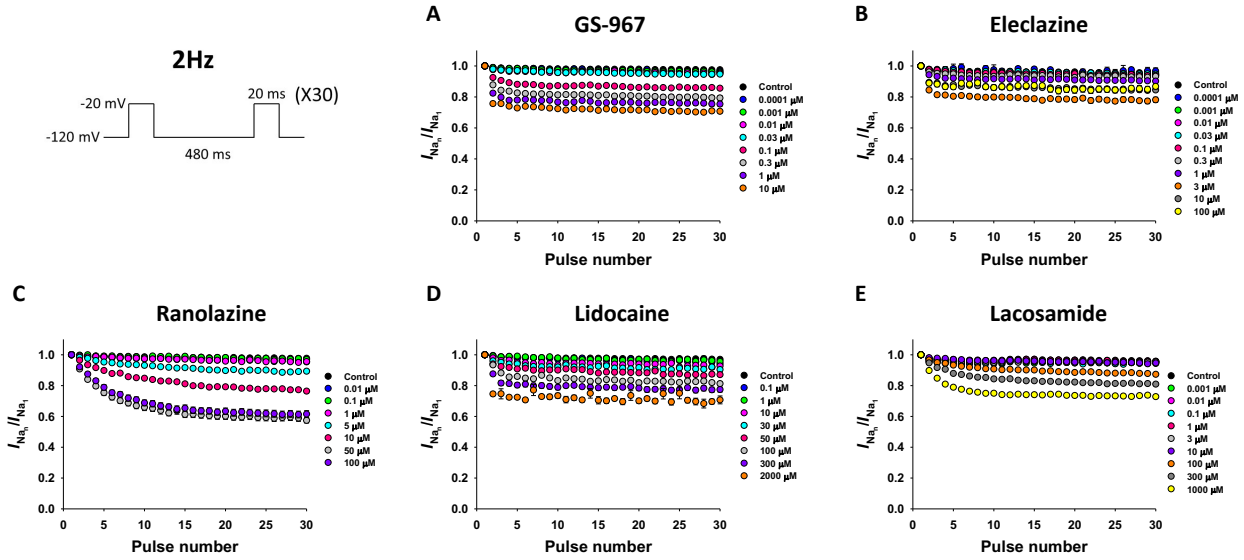

Fig. S2. Use-dependent block of I_{NaP} in human iPSC-derived cardiomyocytes. To examine use-dependent block, cells were held at -120 mV and pulsed to -20 mV for 20 ms at 2 Hz, with an inter-pulse potential of -120 mV (see inset). The peak currents elicited by each pulse were normalized to the peak current of first pulse and plotted against the pulse number. Black symbols represent absence of drug (control), while colored symbols represent experiments in the presence of different concentrations of the drugs tested. **A,** I_{NaP} UDB response to GS-967 (0.0001 - 10 μM); n = 56-100. **B,** I_{NaP} UDB response to eleclazine (0.0001 - 100 μM); n = 4-76. **C,** I_{NaP} UDB response to ranolazine (0.01 - 1000 μM); n = 3-36. **D,** I_{NaP} UDB response to lidocaine (0.1 - 2000 μM); n = 7-22. **E,** I_{NaP} UDB response to lacosamide (0.001 to 1000 μM); n = 37-150. All data are presented as mean ± SEM (for clarity).

SUPPLEMENTAL MATERIAL

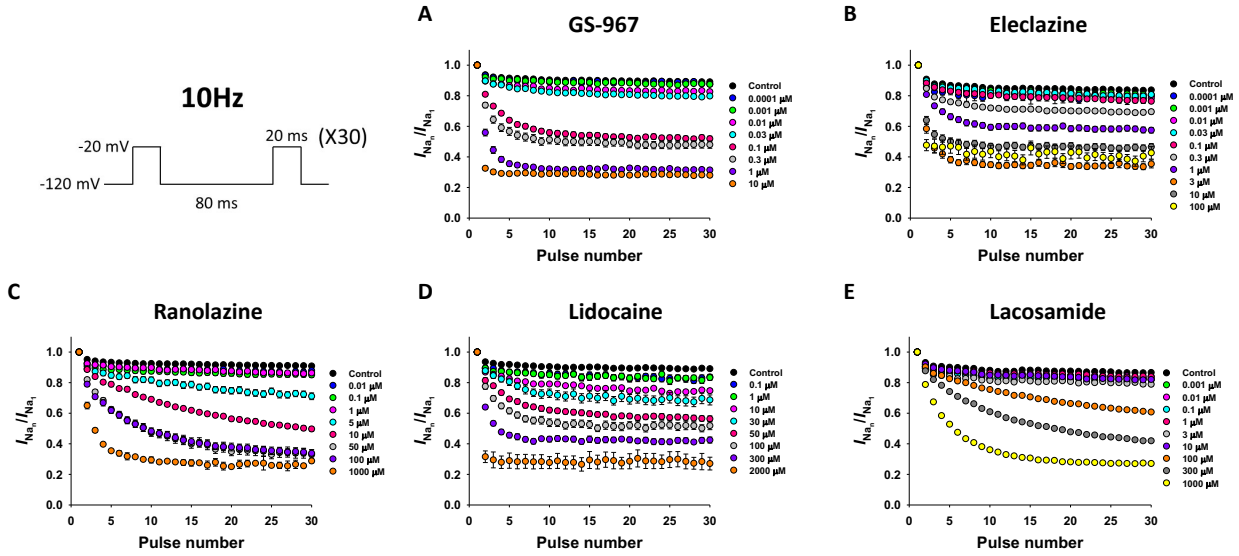

Fig. S3. Use-dependent block of I_{NaP} in human iPSC-derived cardiomyocytes.
To examine use-dependent block, cells were held at -120 mV and pulsed to -20 mV for 20 ms at 10 Hz, with an inter-pulse potential of -120 mV (see inset). The peak currents elicited by each pulse were normalized to the peak current of first pulse and plotted against the pulse number. Black symbols represent absence of drug (control), while colored symbols represent experiments in the presence of different concentrations of the drugs tested. **A,** I_{NaP} UDB response to GS-967 (0.0001 - 10 μM); n = 53-91. **B,** I_{NaP} UDB response to eleclazine (0.0001 - 100 μM); n = 4-64. **C,** I_{NaP} UDB response to ranolazine (0.01 - 1000 μM); n = 2-34. **D,** I_{NaP} UDB response to lidocaine (0.1 - 2000 μM); n = 6-21. **E,** I_{NaP} UDB response to lacosamide (0.001 - 1000 μM); n = 39-144. All data are presented as mean ± SEM (for clarity).

SUPPLEMENTAL MATERIAL

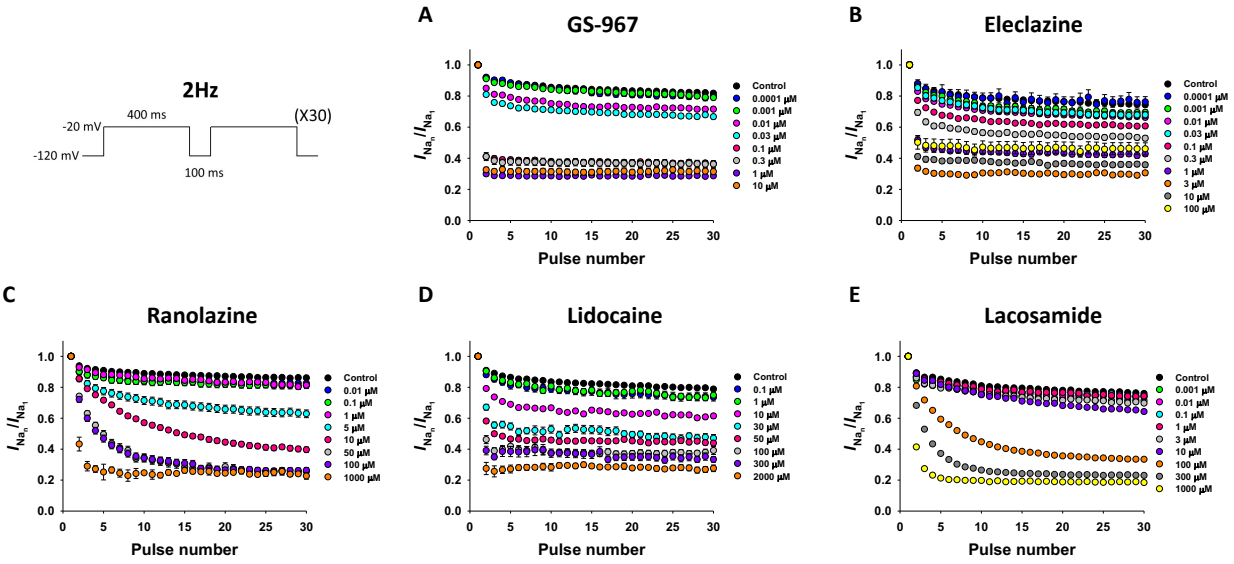

Fig. S4. Use-dependent block of I_{NaP} in human iPSC-derived cardiomyocytes.
To examine use-dependent block, human iPSC-derived cardiomyocytes were held at -120 mV and pulsed to -20 mV for 400 ms at 2 Hz, with an inter-pulse potential of -120 mV (see inset). The peak currents elicited by each pulse were normalized to the peak current of first pulse and plotted against the pulse number. Black symbols represent absence of drug (control), while colored symbols represent experiments in the presence of different concentrations of the drugs tested. **A,** I_{NaP} UDB response to GS-967 (0.0001 - 10 µM); n = 42-79. **B,** I_{NaP} UDB response to eleclazine (0.0001 - 100 µM); n = 4-76. **C,** I_{NaP} UDB response to ranolazine (0.01 - 1000 µM); n = 2-35. **D,** I_{NaP} UDB response to lidocaine (0.1 - 2000 µM); n = 6-22. **E,** I_{NaP} UDB response to lacosamide (0.001 -1000 µM); n = 38-145. All data are presented as mean ± SEM (for clarity).

SUPPLEMENTAL MATERIAL

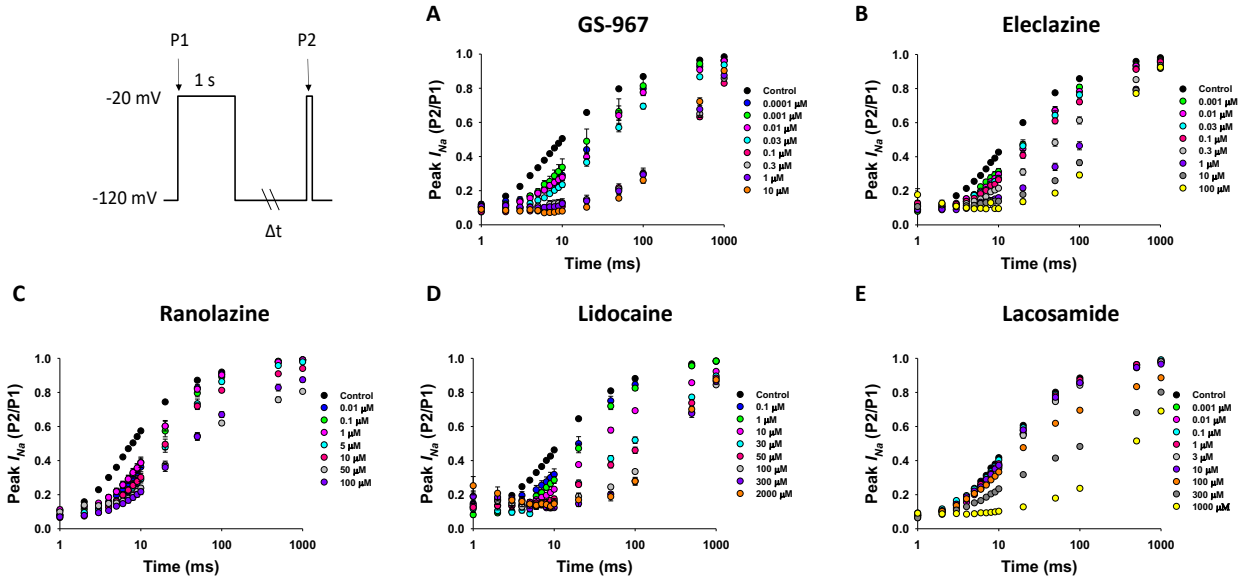

Fig. S5. Effect of GS-967, eleclazine, ranolazine, lidocaine and lacosamide on recovery from inactivation in hiPSC-derived cardiomyocytes.

Recovery from inactivation in hiPSC-derived cardiomyocytes was studied by utilizing a standard two-pulse protocol consisting of a depolarizing (-20 mV) 1000 ms pulse to engage slow inactivation, followed by a variable duration recovery step to -120 mV and a final test pulse (-20 mV, 20 ms); see inset. Channel availability after the end of the recovery interval (P2) was normalized to initial value (P1) and plotted against the recovery time. Recovery from inactivation was determined in the absence (black symbols) or presence of different concentrations (colored symbols) of GS-967, eleclazine, ranolazine, lidocaine and lacosamide. **A,** Recovery from inactivation response to GS-967 (0.0001 - 10 µM); n = 6-27. **B,** Recovery from inactivation response to eleclazine (0.001 - 100 µM); n = 25-40. **C** Recovery from inactivation response to ranolazine (0.01 - 1000 µM); n = 14-30. **D,** Recovery from inactivation response to lidocaine (0.1 - 2000 µM); n = 5-17. **E,** Recovery from inactivation response to lacosamide (0.001 -1000 µM); n = 33-127. All data are presented as mean ± SEM.

SUPPLEMENTAL MATERIAL

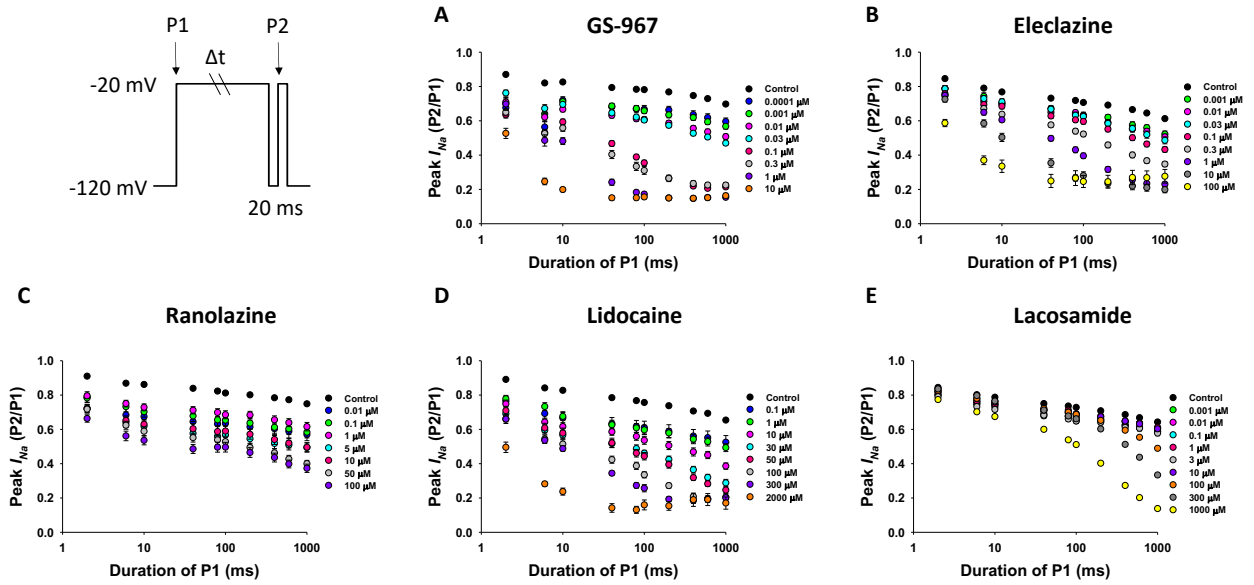

Fig. S6. Effect of GS-967, eleclazine, ranolazine, lidocaine and lacosamide on onset of slow inactivation in hiPSC-derived cardiomyocytes.

Onset of slow inactivation was determined in the absence (black symbols) and presence of different drug concentrations (colored symbols) using a two-pulse protocol (inset): hiPSC-derived cardiomyocytes were held at -120 mV and then depolarized to -20 mV for a variable duration (2-1000 ms) followed by a brief recovery pulse (-120 mV for 20 ms) and a final 20 ms test pulse to -20 mV. Channel entering slow inactivation were estimated by normalizing to initial values (current recorded at P1) the current obtained after the short recovery pulse (current recorded at P2) and plotted against the first pulse duration. **A,** Onset of slow inactivation response to GS-967 (0.001 - 10 µM); n = 11-84. **B,** Onset of slow inactivation response to eleclazine (0.001 - 100 µM); n = 33-72. **C,** Onset of slow inactivation response to ranolazine (0.01 - 1000 µM); n = 5-33. **D,** Onset of slow inactivation response to lidocaine (0.1 - 2000 µM); n = 6-22. **E,** Onset of slow inactivation response to lacosamide (0.001 - 1000 µM); n = 38-140. All data are presented as mean ± SEM.